# Analysis of Murine Polyomavirus DNA Replication:  Large T-Antigen Interaction with Host DNA Damage Repair Protein RPA During Cellular Infection

Katherine E. Rose

University of Colorado Boulder

College of Arts and Sciences

Department of Molecular, Cellular, and Developmental Biology

Defended: April 1st, 2019

Honors Thesis Advisor:

Robert Garcea, MD ǀ Department of Molecular, Cellular, and Developmental Biology

Honors Committee Members:

Christy Fillman PhD | Department of Molecular, Cellular, and Developmental Biology

Robert Garcea MD | Department of Molecular, Cellular, and Developmental Biology

Valerie McKenzie PhD | Department of Ecology and Evolutionary Biology

Molecular, Cellular & Developmental Biology
UNIVERSITY OF COLORADO BOULDER

**Table of Contents:**

## Abstract:

Murine Polyomaviruses are dsDNA viruses that hijack the host's DNA damage response (DDR) pathway to replicate their own genomes (Heiser et al., 2016), offering a model for human polyomavirus replication.  The viral protein large T-antigen (LT) is essential for viral replication and can interact with a variety of DDR proteins in viral DNA replication centers (Brodsky & Pipas, 1998).  Replication protein A (RPA) is a DDR protein complex made up of three subunits, RPA70, RPA32, and RPA14. RPA70 and RPA32 have been shown to directly interact with LT in cells over-expressing each protein, either individually or together (Banerjee et al., 2013). Individual point mutations within LT could disrupt the LT-RPA interaction (Banerjee et al., 2013). However, the LT–RPA interaction has yet to be explored in the context of viral infection.  This study aimed to evaluate mCherry-tagged RPA32 binding with wild-type LT and previously characterized point-mutants E320A and K308E during infection of mouse fibroblasts (Banerjee et al., 2013).  We show that, vDNA was replicated from genomes encoding both wild-type and mutant LT proteins.  However, we did not observe an interaction between wild-type LT and mCherry-tagged mouse RPA32 (mCh-muRPA32).

# List of Abbreviations:

Ab- Antibody

Ag – Antigen

BME- β-Mercaptoethanol

DDR- DNA damage response (repair)

dsDNA- double-stranded DNA

ECL- enhanced chemiluminescence

EDTA- Ethylenediaminetetraacetic Acid

hpi- hours post infection

HPyV- Human polyomavirus

hsRPA32- human RPA32

IB- Immunoblot

IP- Immunoprecipitation

kb- kilobases

LT- Large Tumor Antigen (T-antigen)

MPyV- Murine polyomavirus

MEF- Mouse embryonic fibroblast

muRPA32- mouse RPA32

MW- molecular weight9119

OBD- Origin Binding Domain

ORI- Viral Origin of Replication

PyV - Polyomavirus

RFP - Red fluorescent protein

RPA- Replication protein A

SDS- Sodium Dodecyl Sulfate

ssDNA- single-stranded DNA

SV40- Simian Virus 40

TAg– T antigen

UI- Uninfected

vDNA- viral DNA

WT- Wild-type

# Introduction:

**Polyomavirus:**

Polyomavirus (PyV) are small nonenveloped dsDNA viruses that contain a circular genome (~5.2 kb) packaged within an icosahedral capsid composed of pentameric proteins (Fanning, Zhao, & Jiang, 2009). Polyomaviruses have a wide host range, infecting both bird and mammals, including fourteen known human viruses (Prado et al., 2018; Topalis, Andrei, & Snoeck, 2013)  Human polyomaviruses been implicated in a variety of human disease, most notably BK Polyomavirus (BKPyV) and JC Polyomavirus (JCPyV), which affect immunocompromised hosts such as transplant recipients and those infected with HIV (Ahsan & Shah, 2006; Topalis et al., 2013).  Due to their widespread nature and the recent discovery of new human strains, PyVs have become a target of research and vaccine development, with efforts aimed at understanding and targeting pathways of viral DNA replication.  Non-human polyomaviruses, particularly Simian Virus-40 (SV40) and murine polyomavirus (MPyV) are studied extensively in hopes of shedding light on the exact molecular mechanisms that contribute to viral replication and spread (Fanning, Zhao, & Jiang, 2009; Heiser et al., 2016)

MPyV is a powerful model of eukaryotic DNA replication, as the genome, like other members of the PyV family, is almost entirely replicated by host cell machinery.  MPyV's entry and replication within mouse cells is thought to parallel that of other polyomaviruses (human) offering researchers the ability to study the mouse virus (which is easy to culture/grow) and translate findings over to.  The genome of MPyV encodes six gene products, separated into 'early' and 'late' regions.  Each "region" is expressed at different times in the viral life cycle (**Figure 1**)(Fanning et al., 2009) .  These distinct phases in viral transcription are a result of two separate transcriptional units within the PyV genome; each being transcribed in the opposite direction of the other (Fanning et al., 2009). In addition, each circular genome contains an

origin, bidirectional enhancer region, and promoters for the early and late transcriptional units (Fanning et al., 2009).

Three 'early' products make up a group of viral proteins, referred to as tumor antigens (TAg), called small, middle, and large TAgs (Brodsky & Pipas, 1998). The expression of these proteins is mediated by host transcriptional factors early in infection (Fanning et al., 2009). Small and middle TAg (ST and MT) have been shown to play roles in host-protein phosphorylation and kinase signaling pathways within the host cell upon infection (Andrabi et al., 2007; Fluck & Schaffhausen, 2009). Large TAg (LT) is directly involved with viral DNA replication (Brodsky & Pipas, 1998;Topalis et al., 2013).

Late transcriptional products include the viral capsid proteins; VP1, VP2, and VP3 (Brodsky & Pipas, 1998). VP1 is a major viral capsid protein of ~45kD, forming pentamers through interactions at their C-terminus which in turn make up the majority of polyomavirus's icosahedral structure (Stehle & Harrison, 1997). At the center of each VP1 pentamer is a single copy of either one of the minor capsid proteins VP2 and VP3, which function as a point of contact between the viral capsid and the condensed mini chromosome of vDNA (Fanning et al., 2009).
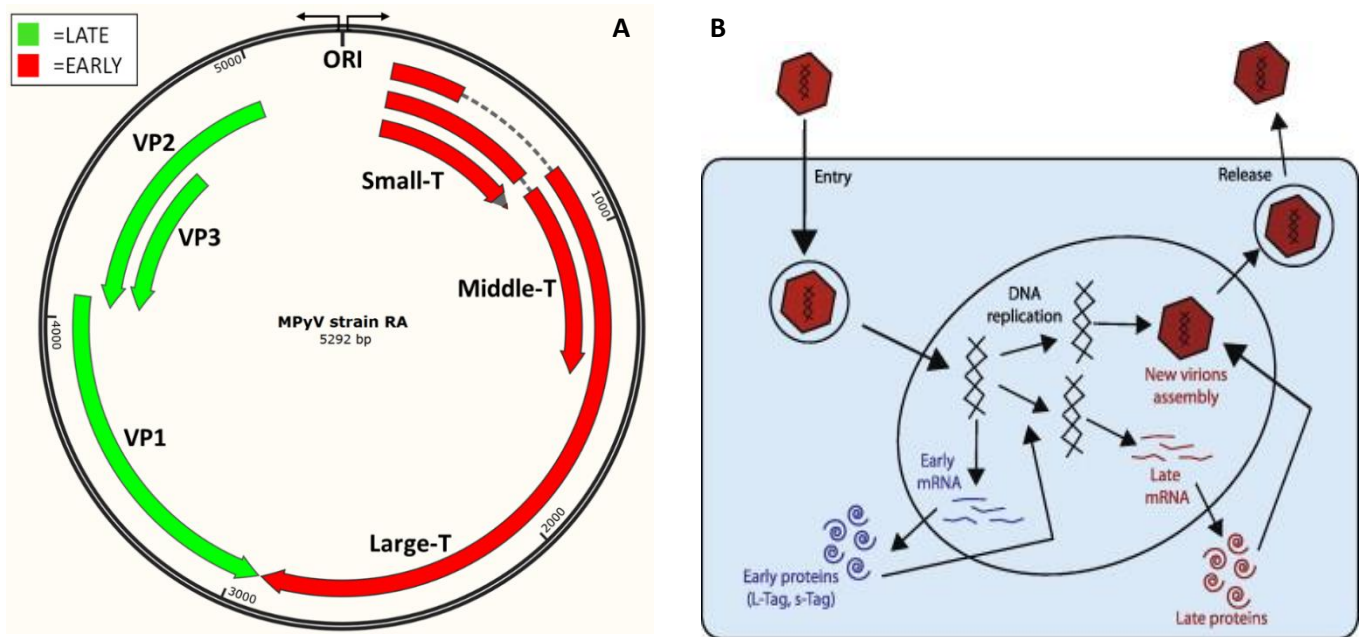
**Figure 1: MuPyV genome and life cycle. (A)** MPyV proteins are grouped into 'Early' and 'Late' categories based on their function/transcriptional order. Early proteins (Red) consist of small, middle, and large tumor-antigens (TAg). These working the early stages of viral replication, recruiting host cell machinery and facilitation DNA replication. Late proteins (Green) form the viral capsid; Viral proteins (VP) 1/2/3. **(B)** Polyomaviruses replicate within the host cell nucleus and undergo two phases. Early transcription (Blue) leads to proteins that contribute to vDNA replication. Late transcription (Red) generates viral capsid proteins (VP1/2/3), and mediate viral assembly. (Figure adapted from Topalis et al., 2013).

## Large T-Antigen

Large Tumor Antigen (LT) is a ~88 kD protein consisting of multiple functional domains; including a helicase domain with ATPase activity, origin binding domain (OBD), and J-domain (**Figure 2**) (Brodsky & Pipas, 1998; Fanning et al., 2009; Topalis et al., 2013). LT oligomerizes into a hexameric structure, forming a ring that allows for the activation of its helicase domains. Each hexamer is responsible for unwinding the dsDNA of the virus (Topalis et al., 2013). Two 'rings' of LT helicase domains associate with the OBD, forming a dodecamer; the OBD in turn



**Figure 2: Structure/domains of Large T-Antigen**. LT consists of a DNA-J domain connected to the OBD via a linker region. The following helicase region in turn associates with the OBD, allowing for activation of its ATPase activity and consequently unwinding of vDNA during DNA replication. Approximate locations of mutants K308E (star ★ ) and E320A (triangle ▲ ) are shown; occurring in the helicase region thought to mediate RPA interaction.

binds to the viral origin (ORI) to regulate vDNA replication (**Figure 3**) (Fanning et al., 2009; Topalis et al., 2013). The OBD recognizes a specific sequence of nucleotides at the ORI, and associates with the negatively-charged backbone of the vDNA via its positive/uncharged amino acids (Topalis et al., 2013). The N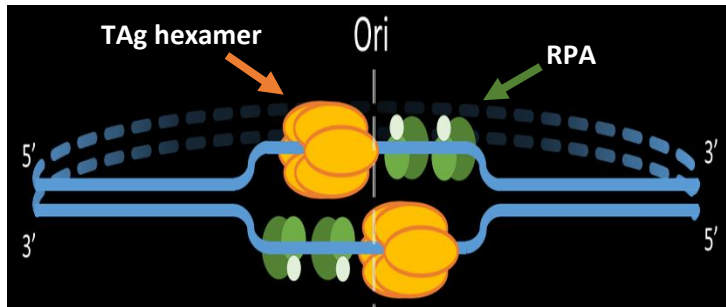-terminus of LT is comprised of DNA-J domain approximately 70 amino acids in length; these domains function as stimulators of DNA-K's, a type of cellular chaperon with ATPase activity (Whalen, de Jesus, Kean, & Schaffhausen, 2005). The formation of LT DNA-J/K chaperon complexes promotes vDNA replication, helping to drive cell cycle progression (Whalen et al., 2005).



**Figure 3: Structure of TAg on PyV replication fork.** TAg hexamers (orange) position themselves on the viral origin (ORI) I via their DNA-binding domains (OBD). TAg hexamers function as helicases to unwind the double-helix bi-directionally along the circular genome. Additionally, TAg associates with various host DDR proteins, including RPA (green) to facilitate efficient viral DNA replication. (Image from Douglas Peters)

LT is essential for infection and replication of viral DNA. LT can mediate cell cycle progression into S-phase through phosphorylation of specific host proteins including the retinoblastoma tumor suppressor (Rb) family (Fanning et al., 2009). The switch to S-phase results in the expression of host cell genes required for DNA synthesis such as CHK2, DNA polymerase α, and thymidine kinase. A prolonged S-phase provides PyV with the necessary host proteins/enzymes required for its own DNA replication (Sullivan & Pipas, 2002). Once in S-phase, transcription of other TAg proteins begins, along with replication of the viral genome. Finally, LT may interact with host proteins, such as DNA polymerase α, primase, topoisomerases, and other DNA-damage response (DDR) proteins at viral DNA replication sites (Brodsky & Pipas, 1998).

MPyV replication centers (places where viral DNA is replicated) are defined using light microscopy by staining for either LT or viral DNA (Figure 4, Garcea lab, unpublished data). Early after infection, replication centers are seen as small punctate "dots" (Figure 4, 24 HPI); as infection progresses, the small dots "merge" into large "tracks" that run throughout the nucleus (Figure 4, 28 and 32 HPI). DDR proteins, such as RPA32, Mre11, CHK1, pATM, and γH2AX are recruited to these locations of viral DNA replication (Heiser et al., 2016).
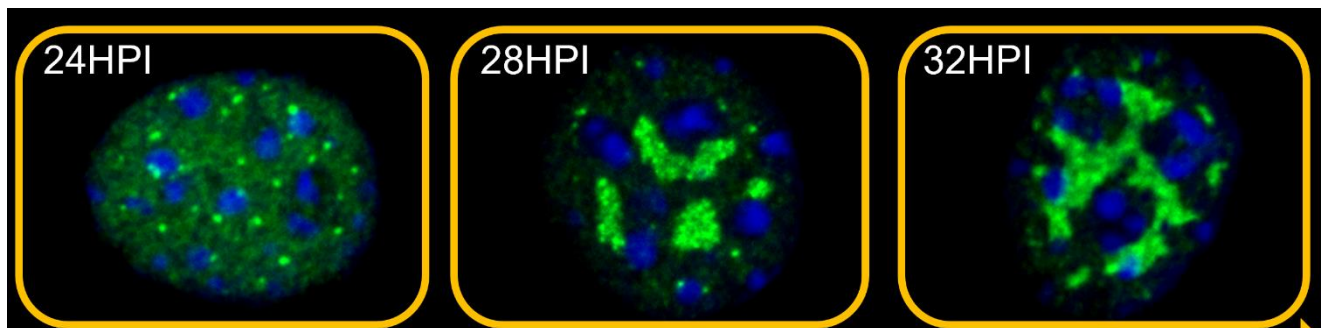


**Figure 4: MPyV replication centers**. MEF C57cells infected with RA were fixed and stained for LT (green) and chromosomal DNA (DAPI, blue) at indicated times. Viral replication centers are visualized by staining for LT. During early times after infection, small LT foci form in the nucleus (24hpi); later during infection, these replication centers spread into long 'tracks' throughout nuclei (28 and 32hpi). (Image courtesy of Doug Peters, unpublished).

**Host Cell DNA-Damage Repair**

Cells are often exposed to a variety of chemicals/environments that result in DNA damage. To survive and replicate, an effective yet robust intracellular system is needed that can both recognize and repair endogenous/exogenous insults. The DNA-damage response pathway in eukaryotic cells utilizes a complex array of proteins and signaling to detect DNA damage and fix breaks in the genome (Jackson & Bartek, 2009). DNA breaks (single and double stranded) are recognized through kinase signaling cascades (ATM and ATR) that ultimately recruit DDR proteins to the site of damage, arresting the cell cycle during the repair process to prevent cells from possibly becoming cancerous (Jackson & Bartek, 2009). Polyomaviruses hijack or alter the DNA repair pathway as a means to further their own

replication, re-directing DDR proteins to sites of vDNA replication  (Banerjee et al., 2013;Fanning, Klimovich, & Nager, 2006; Heiser et al., 2016)

MpyV can hijack and re-direct a host's DDR pathway to productively replicate its genome.  LT may be one factor in the recruitment of DDR proteins to viral replication centers within the nucleus (Banerjee et al., 2013; Brodsky & Pipas, 1998; Heiser et al., 2016; Topalis et al., 2013).  However, the exact signaling pathways/proteins interactions which mediate this DDR protein recruitment remain poorly understood.  While MpyV's reliance on the DDR pathway for replication has been documented, questions remain about the nature of certain LT-host protein binding events and their overall role in viral replication.

Replication Protein A (RPA) acts as a ssDNA binding protein complex at sites of damage, preventing hairpin formation and signaling the DNA-damage response pathway (Fanning et al., 2006).  RPA is a heterotrimeric complex consisting of a 70, 32, and 14 kD subunit (referred to as RPA70, RPA32, and RPA14, respectively);  together this complex helps to regulate not only the DDR, but also DNA replication, and recombination (Banerjee et al., 2013; Fanning et al., 2006; Wold, 1997).  RPA is thought the be recruited to sites of viral replication DNA replication via LT, binding to ssDNA as it is unwound via the helicase domains of LT (Jiang et al., 2006).  The OBD of LT hexamers associate with the C-terminus of the RPA32 subunit, allowing for loading of the polymerase/primase complex onto the vDNA (Fanning et al., 2009; Jiang et al., 2006).  This binding interaction, and resulting RPA subunit remodeling, mimics that of other DDR proteins in a host cell; LT interacts with the same binding face of RPA32 used by other repair proteins (Fanning et al., 2006).

Research suggests LT and RPA interact to effectively replicate viral DNA during infection (Banerjee et al., 2013).  The mode of interaction between LT and RPA70  (via its N-terminus) is thought to mimic interactions of RPA and other host DDR proteins during DNA damage (Ning et al., 2015).  Additionally, a direct association between RPA70 and LT has been

observed using co-immunoprecipitation (Banerjee et al., 2013). LT with single point mutants E320A and K308E, did not co-immunoprecipitate with GFP-RPA70, suggesting that they are defective in their ability to bind RPA (Banerjee et al., 2013). However, the exact effect of these LT mutants on the process of viral DNA replication has not been explored.
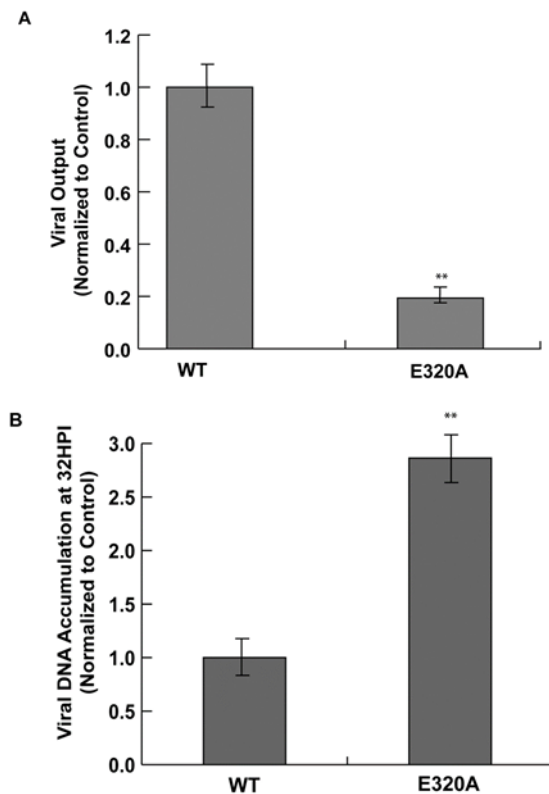


**Figure 5: Comparison of viral output and DNA replication in E320A mutant.** (**A**) Mutation at the 320th residue of LT significantly decreases overall viral output during infection when compared with WT. However, viral DNA levels (accumulation) after 32 hours appear to be significantly higher in the TAg mutant (**B**), indicating the virus may not be able to effectively replicate/package its DNA. (Figure from Katie Heiser, Garcea Lab unpublished)

Since the interaction of LT and RPA was examined using cells transfected with expression plasmids for individual genes, we wanted to explore the LT-RPA interaction in mouse cells infected with MPyV. To this end, we generated LT mutants that contain each single point mutation, (E320A and K308E), and a double mutant (E320A + K308E) in the context of the viral genome (**Figure 3, star and triangle**). Previous unpublished work from the Garcea lab using vDNA encoding the E320A mutation in LT suggests this mutation results in decreased viral titer, but higher levels of overall vDNA replication (**Figure 5**) (Garcea Lab, unpublished). It was hypothesized that replication of vDNA by E320A LT resulted in aberrant replication and "unpackagable" concatamers of vDNA.

To study the interaction of LT and RPA when the mutations are expressed in the context of the viral genome, we used mouse fibroblast cells that stably express an mCherry-tagged mouse RPA32 (mCh-muRPA32). I will present data that shows that the transfection of the viral genome is efficient, and the LT mutants can

replicate viral DNA.  Additionally, I will show that LT does not co-immunoprecipitate with mCh-

muRPA32 in our system.  Implications and differences with previous studies will be discussed.

## Materials and Methods

### Cell culture

C57 are mouse embryonic fibroblasts (MEF) and C57 lines that stably-express an mCherry-tagged RPA32 protein were used for all infections and transfection experiments.  Cells were grown in Dulbecco's Modified Eagle's Medium (DMEM) supplemented with10% fetal bovine serum (FBS), 1% penicillin-streptomycin solution (P/S), and 60uM β-Mercaptoethanol (BME) and grown in a humidified environment at 37°C with 5% $CO_2$.

### Virus and Infections

NG59RA is wild-type MuPyV.  Cells to be infected were grown to 50% confluency; growth media was removed and replaced with starve medium (DMEM/BME/P/S without serum) prior to infection.  Viral supernatant was prepped using sonication (65 watts, 1 min), heated at 45°C for 15 min and cellular debris was pelleted by centrifugation. The supernatant was removed and diluted in adsorption buffer (1% bovine calf serum/1X Hank's serum/10mM Hepes, pH 5.6).  Starve media was removed from plates, virus was added to cells and incubated at 37°C, 5% $CO_2$ for one hour.  After incubation, virus was removed, replaced with growth media, and incubation continued for 28-32 hours.

### Mutagenesis

The NG59RA virus genome was cloned into pUC18 at BamHI sites (pUC-RA; Katie Heiser); this plasmid was used to generate mutations within the LT sequence. The E320A mutation was made by a previous Garcea lab member (pUC-E320A).  Both

pUC-RA and pUC-E320A plasmids were confirmed by sequencing prior to further

mutagenesis.

Single nucleotide mutants (K308E) and the double mutant (E320A+K308E) were

generated using a QuikChange II XL site-directed mutagenesis kit per manufacturer

protocol.  For single (K308E) mutants, pUC-RA was utilized; for the double-mutant

(E320A+K308E), pUC-E320A.  The same mutagenic primers were used for each

plasmid. K308E-forward:  5'ctcatgctatttattctaatgaaacgttcccggcatttctagtatactcc3'; K308E-

reverse: 5'actagaaatgccgggaacgtttcattagaataaatagcatgagacaaataccc3'; the single

nucleotide mutation is underlined. Mutagenic reactions were incubated in a

thermocycler as follows: 95°C (50 sec), 60°C (50sec), and 68°C (7 min), for a total of 18

cycles. Reactions were transformed into XL10-Gold ultracompetent cells, plated on LB-

Ampicillin plates, and grown overnight at 37°C.  Colonies were screened by PCR colony

check and positive clones were isolated, grown up for large scale isolation and

confirmed by sequencing.

**Hirt DNA Isolation**

Media was removed from transfected (RA, K308E, E320A, E320A+K308E) and

UI plates and washed with ice-cold PBS (Phosphate-buffered saline).  Lysis buffer

(0.01M Tri-HCL, pH 7.4 / 0.01M EDTA / 0.6% SDS) was added to the plates and

incubated for 10-20min (at room temperature) before being scraped into tubes.  To this,

¼ volume 1M NaCl was added before overnight incubation at 4°C.  The following day,

samples were centrifuged at 14,000xg for 30 min to sediment cellular DNA, and the

supernatant was transferred to new tubes.  RNase A was added to the supernatant and

samples were incubated at 37°C for 30 min, followed by incubation with proteinase K at

37°C for 45 min.  Samples were phenol-chloroform extracted one time and then DNA was ethanol precipitated. The precipitated DNA was pelleted by centrifugation (14,000xg) and washed with 70% EtOH and allowed to dry.  The DNA pellet was re-suspended in 1X TE (10mM Tris / 1mM EDTA) and stored at -20°C until use. Concentrations of each sample were determined by $OD_{260}$.

## Transfections

Prior to transfection plasmids encoding the viral genome with or without mutations (pUC-RA, pUC-E320A, pUC-K308E, pUC-E320A+K308E) were prepared by restriction digest with BamHI to linearize and excise the viral genome from the pUC plasmid (**Figure 6**).

Digested samples were cleaned up using New England Biolabs Monarch DNA clean-up kit.  Linearized DNA was used in all transfection experiments.  $5 \times 10^5$ cells per transfection were collected by centrifugation (400xg) and re-suspended per manufacturer protocol for the Nucleofector IIb, Mouse Embryonic Fibroblast Nucleofector Kit 1 (VDP-1004, Lonza).  Digested and cleaned DNA was added to the cell suspension and electroporated using the program T020 on the Nucleofector IIb device. The transfected cells were resuspended in growth media and processed as described for the appropriate assay.  Cells were incubated at 37°C, 5% $CO_2$, until ready to harvest.

## Lysates for IP/Westerns

Cells were washed with cold PBS, scraped from flask, and pelleted via centrifugation (1000 xg).  Cells were lysed using Lysis Buffer (20mM Tris, pH 7.5 / 150mM NaCl / 1mM EGTA / 1mM EDTA / 1% Triton x-100) plus protease and

phosphatase inhibitors, and incubated 30min room (mini-Complete protease cocktail inhibitor / 2mM Sodium Vanadate / 5mM Sodium Fluoride).  Lysates were clarified via centrifugation at 4°C.  Supernatants were stored at -20°C until use.

**Immunoplaque Assay**

Immediately following transfections, aliquots of each diluted transfection were plated on a 96-well imaging plate final cell density of 5000 cells per well and incubated at 37°C, 5% $CO_2$.  Each transfection was plated in quadruplicate.  At 28 hpi, the culture media was removed, and cells were fixed with 4% paraformaldehyde) (PFA) in PBS before being permeabilized with 0.5% Triton X-100.  A solution of 5% fetal bovine serum (FBS) in PBS was used to block cells overnight at 4°C.  Cells were incubated with anti-TAg primary antibody (E1; T. Benjamin) at a 1:2500 dilution, 1 hour at 37°C.  Cells were washed with FBS/PBS three times and incubated with goat anti-rat AlexaFluor-488 conjugated secondary antibody (1:2500, LifeTechnologies) and Hoescht dye (1:2500) for 45 minutes at 37°C in the dark.  Secondary antibody/Hoescht was removed, replaced with PBS, and the plate was kept at 4°C in the dark until imaged.  Plates were imaged on a Molecular Devices ImageXpress XL High-Content Screener.


**Transfection Efficiency Analysis**

Images taken from 96-well plates were analyzed for total cell count along with number of LT-positive (infected) cell nuclei.  MATLAB script was designed and provided by Doug Peters.  For images of wells with multi-nucleated cells (resulting from transfection process) hand-counting of nuclei and infected cells was undertaken, since MATLAB script could not differentiate as distinct nuclei.  The percentages of LT-positive

cells per DNA concentration was calculated by dividing the number of LT-positive nuclei by the total number of nuclei within a well. Standard deviation of each set of triplicates was determined

**Immunoprecipitation for T-antigen**

C57s stably expressing either mCherry-tagged hsRPA32 or muRPA32 were infected with NG59RA at a 1:50 dilution, as described above.  At 28-30 hpi, Cells were washed with cold PBS, scraped from flask, and pelleted via centrifuge.  Pelleted cells were lysed by incubating in Lysis Buffer (20mM Tris, pH 7.5 / 150mM NaCl / 1mM EGTA / 1mM EDTA / 1% Triton x-100) plus protease and phosphatase inhibitors on ice for 30 min before clarification via centrifugation.  An aliquot of the total cell lysate was removed prior to immunoprecipitation and acted as the INPUT sample for each experiment.

To make anti-TAg- bead complexes, 50ul protein G magnetic Dynabeads (Invitrogen) were washed once with lysis buffer.  Washed Beads were incubated with 2ug anti-TAg antibody diluted in lysis buffer + inhibitors and incubated at room temperature for 1 hour.  After incubation, bead-Ab complexes were washed three times with lysis buffer.

Cell lysates incubated with either bead-Ab complexes or 25ul washed RFP-Trap magnetic beads (RTMA-10, ChromoTek) with rotation, overnight at 4°C.  Samples were washed three times with lysis buffer. The supernatants from the overnight incubation (POST IP) and first wash (WASH 1) were saved and combined with an equal volume of 4X SDS sample buffer (200 mM Tris, pH 6.8 / 2% SDS / 40% Glycerol / 700 mM BME / 0.02% Bromophenol Blue.  Washed beads were re-suspended in 50ul 2X SDS sample

buffer (100 mM Tris, pH 6.8 / 1% SDS / 20% Glycerol / 350 mM BME / 0.01% Bromophenol Blue) (IP).

**Western blotting**

Samples were boiled for 5 min to denature and separate the proteins from beads. 10ul IP and 20ul INPUT/POST IP SN/WASH1 samples were resolved on 10% SDS polyacrylamide gels at 125V constant volts.  Protein were transferred to PVDF at 4° at 50V constant voltage for two hours.  Membranes were blocked overnight (4°C) in 5% milk/1X TBST (TBS/0.05% Tween 20).  Blots were stained with antibodies to either LT (1:100; PN116, B. Schaffhausen), mCherry (1:1000; 632496, TaKara), or RPA32 (1:5; 4E4, H. Nasheuer) by incubating overnight at 4°C with rocking.  Membranes were washed three times with 1X TBST, incubated with appropriate HRP-conjugated secondary antibodies, and proteins detected by enhanced chemiluminescence (ECL, Promega). Antibodies were stripped by incubating in Stripping Buffer (0.1M Glycine / 0.01% Tween 20 / 0/1% SDS / pH 2.2) for 20min at room temperature, followed by three washes of dH$_2$O and an additional three washes in 1X TBST.  Stripped blots were blocked in milk and re-probed for as indicated according to the above protocol.

# Results

## Transfection efficiency of linearized DNA

The transfection efficiency of C57 cells was determined to optimize protocol for use in future experiments.  To ascertain the optimal amount of vDNA to transfect, increasing concentrations of DNA were tested.  Traditionally, viral genomes are isolated from pUC plasmids and re-ligated to make complete circular genomes.  However, this requires large amounts of plasmid DNA (50ug) and large volumes for the ligation.  We wanted to test if we could bypass these restrictions by using linearized vDNA isolated from pUC plasmids digested with BamHI (**Figure 6**).  Additionally, we wished to test if
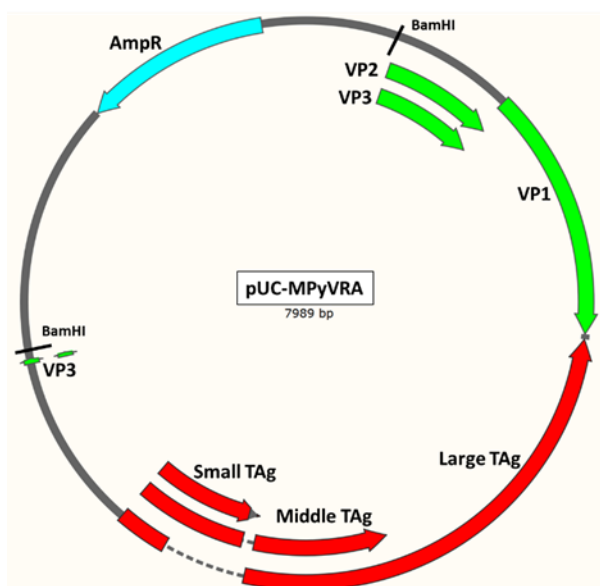


**Figure 6: pUC plasmid with MPyV genome.** BamHI sites used for digests indicated.  pUC plasmids used for WT and LT mutants contained an ampicillin resistance gene.

linearized vDNA could result in DNA replication. Transfected cells were assayed for TAg expression using an immunoplaque assay developed in the Garcea lab. The percentage of TAg-positive cells was determined for each sample.  Transfection efficiencies for digested pUC-RA and each pUC-LT mutant varied considerably, ranging from <5% to 20% of cells positive for TAg expression (**Table 1**).  Cells transfected with increasing amounts of

vDNA had typically higher percentages of TAg positive cells.  For the purpose of future experiments, linearized vDNA was used in all transfections.

**Table 1: Transfection efficiency of linearized viral genomes[1]**

| vDNA (ug) | pUC-RA | E320A | K308E | E320A+K308E |
|---|---|---|---|---|
| 2.5 ug | 3.7±1.2 % | 1.5±0.2% | 1.0±1.2% | 13.0±0.5% |
| 5.0 ug | 7.75±2.5% | 5.5±1.0% | 15.0±3.1% | 16.0±2.2% |
| 7.5 ug | 6.75±2.9% | 3.0±1.8% | 18.0±2.9% | 8.75±5.0% |

[1] percentage of TAg positive cells with standard deviation

## Mutant vDNA can be replicated after transfection

To determine whether viral DNA is replicated when mutant LT proteins are expressed, C57 cells were transfected with linearized vDNA as described above. At 48hpi, cells were lysed and viral DNA was isolated by the method of Hirt (Hirt, 1967). The presence of replicated viral DNA was analyzed by agarose gel electrophoresis.

Cells transfected with linearized viral DNA resulted in vDNA replication 48 hours post transfection (**Figure 7**). There appears to be no difference in band intensity based on amount of vDNA initially transfected into cells (**Figure 7**), however, since we did not perform an immunoplaque assay of the percent of LT positive, we cannot make a conclusion about the relative amounts of replicated DNA.
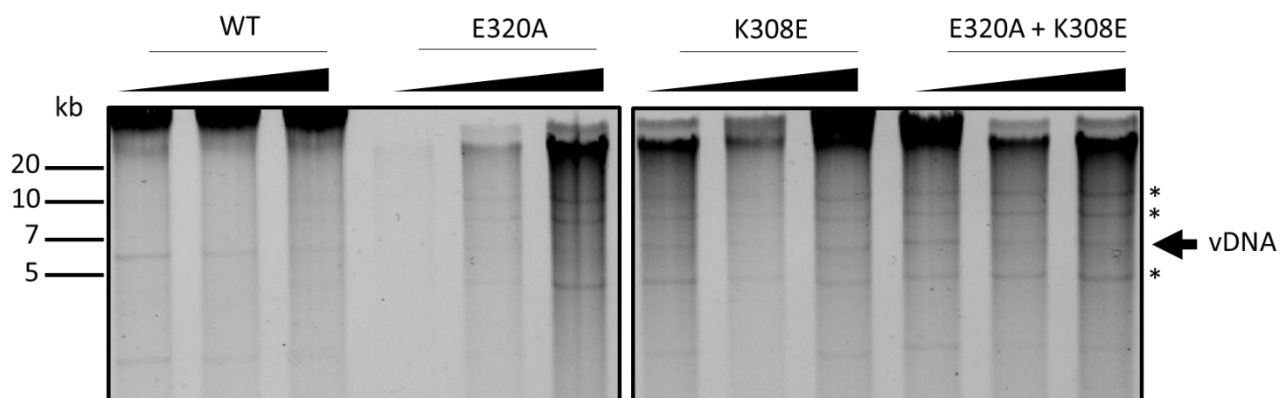


**Figure 7: DNA gel of HIRT isolated DNA from mutant transfected samples.** Bands indicating the presence of viral DNA are visible at ~5.2 kb, suggesting viral DNA replication. Cells were transfected with either 2.5, 5, or 7.5 ug of DNA; plates were harvested 48hpi and vDNA was isolated and linearized by BamHI digestion. Samples were resolved by 1% agarose gel electrophoresis. Asterisks (*) indicates bands of unknown origin seen some lanes.

Overall, vDNA can be visualized in all samples (cells) following transfection with either WT or mutant DNA. Each LT mutant, apart from lower initial starting amounts of E320A, replicated vDNA. It is interesting to note that that cells transfected with the mutant DNA showed multiple DNA bands regardless of the transfected amount of DNA. These extra bands were not seen in cells transfected with WT DNA and it is unclear what these extra DNA bands represent (**Figure 7**).

## mCherry-RPA23 can be immunoprecipitated

RFP-trap is a method of one-step immunoprecipitation for RFP- fusion proteins and their interacting factors. Single heavy-chains of alpaca antibodies, nanobodies, specific for RFP fusion variants are coupled to magnetic beads. We wanted to test the ability of RFP-traps (ChromoTek) to immunoprecipitate (IP) mCherry-tagged RPA32. Cell lysates from C57 mouse fibroblasts that stably express and mCherry-tagged mouse RPA32 (mCh-muRPA32) were either mock infected or infected with wild-type MPyV (NG59RA). Samples were evaluated by immunoblot analysis using a pan-antibody that recognizes any RFP tag.
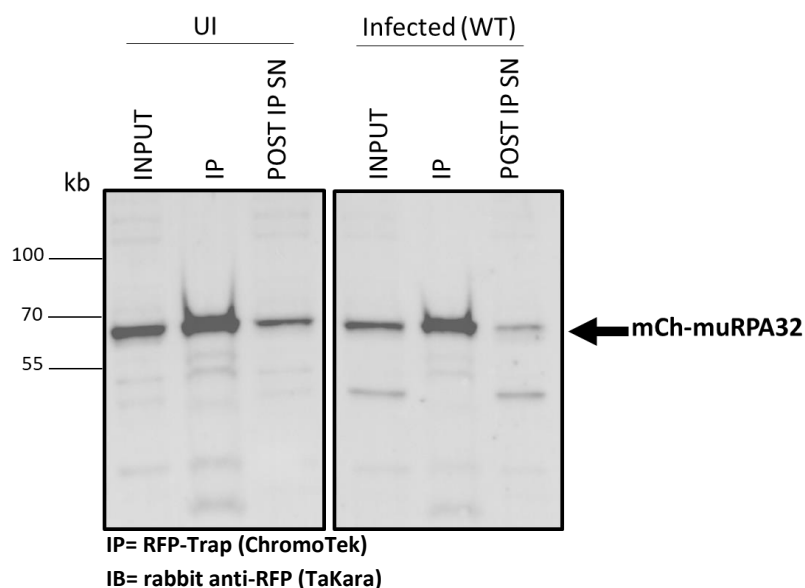


**Figure 8: Immunoprecipitation using RFP-trap effectively pulls down mCherry tag**. Cells were infected with WT (RA) and harvested 28-32 hpi. Cell lysates were incubated with RFP-trap columns to IP mCh-muRPA32. Samples were resolved on an SDS polyacrylamide gel and blotted for mCh-muRPA32 using anti-RFP antibody. INPUT represents 5% of the starting cell lysate; IP, protein that bound to the RFP-trap; POST IP SN, supernatant from the IP and contains proteins that did not bind to the RFP-trap.

mCh-muRPA32 was immunoprecipitated from both infected and UI cells using the RFP-trap columns (**Figure 8**).  A band that migrates at the correct molecular weight (~67 kD) is seen in all samples assayed, with an enrichment in the IP sample (**Figure 8**). Additionally, the POST IP SN lanes of each sample show less protein, indicating that most of the mCh-muRPA32 within the cell lysates was bound to the RFP-trap.

## Large TAg and mCh-muRPA32 do not coimmunoprecipitate

To determine if LT and RPA32 can bind one another and co-precipitate, two co-IP experiments were performed; one IP for LT and the other using RFP-trap to pull down mCh-muRPA32.  The LT IP samples were analyzed by immunoblot with antibodies to mCherry, while the RFP-trap samples were blotted for LT.  These would indicate if both proteins are able to co-immunoprecipitate one another in the context of infection. We wished to test this interaction under similar conditions to those where a LT-PA70 interaction observed (Banerjee et al., 2013).  Cells stably expressing mCh-muRPA32 were either infected with WT polyomavirus (NG59RA) or left uninfected and harvested 28-30hpi.  Cell lysates were generated and incubated with Ab-bead complexes as described.  Samples were resolved by SDS polyacrylamide electrophoresis and immunoblotted for the indicated protein. Blots were stripped and re-probed as indicated to confirm that the IP was successful.

Lysates from infected mCh-muRPA32 cells did not co-IP LT.  When LT was IP'd, we did not observe mCh-muRPA32 in infected samples when blots were probed for mCherry or RPA32. (**Figure 9A, C**).  However, when blots were stripped and re-probed with anti-TAg, bands corresponding to LT were present in the 'IP' (**Figure 9B**).
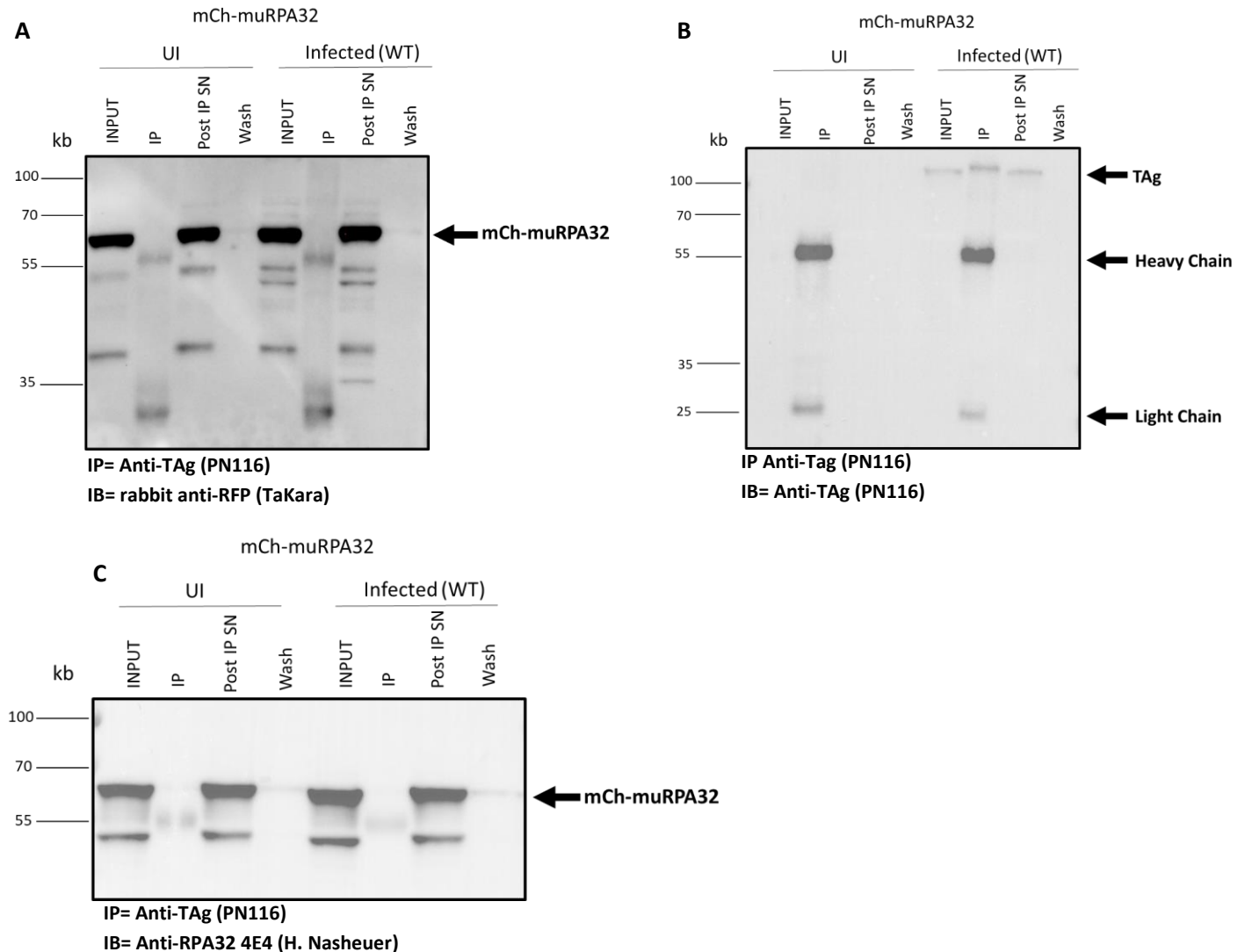
**Figure 9: RPA32 does not co-immunoprecipitate with LT in the context of infection.** C57 cells stably expressing mCh-muRPA32 were infected with NG59RA. At 30 hpi, cells were lysed, and LT was immunoprecipitated. Samples were analyzed by immunoblot with antibodies indicated. Blot **A** was blotted and imaged, the antibodies stripped, the blot and re-probed as indicated **(B)**. **(A)** Samples IP'd for LT and blotted with anti-mCherry antibody **(B)**. Blot A was stripped and re-probed for LT (indicated with an arrow); since it is the same antibody that was used for the IP, we observe the heavy and light chains of the IP antibody. **(C)** Samples were IP'd for LT and blotted for with anti-RPA32 antibody. INPUT= 5% of the whole lysate, IP= final precipitated protein, POST IP SN= supernatant following IP incubation, WASH= first Lysis Buffer wash of Ab-bead complexes

Lysates IP'd using RFP-trap yielded similar results; when blots were probed with anti-TAg, no LT was present in the IP of infected cells and was instead observed in the POST IP SN (**Figure 10A**). Alternatively, bands indicating the presence of mCh-

muRPA32 were seen when probed for mCherry or RPA32 (**Figure 10B, C**).  These data

indicate that while each IP worked at pulling down its target protein, LT and RPA32 did
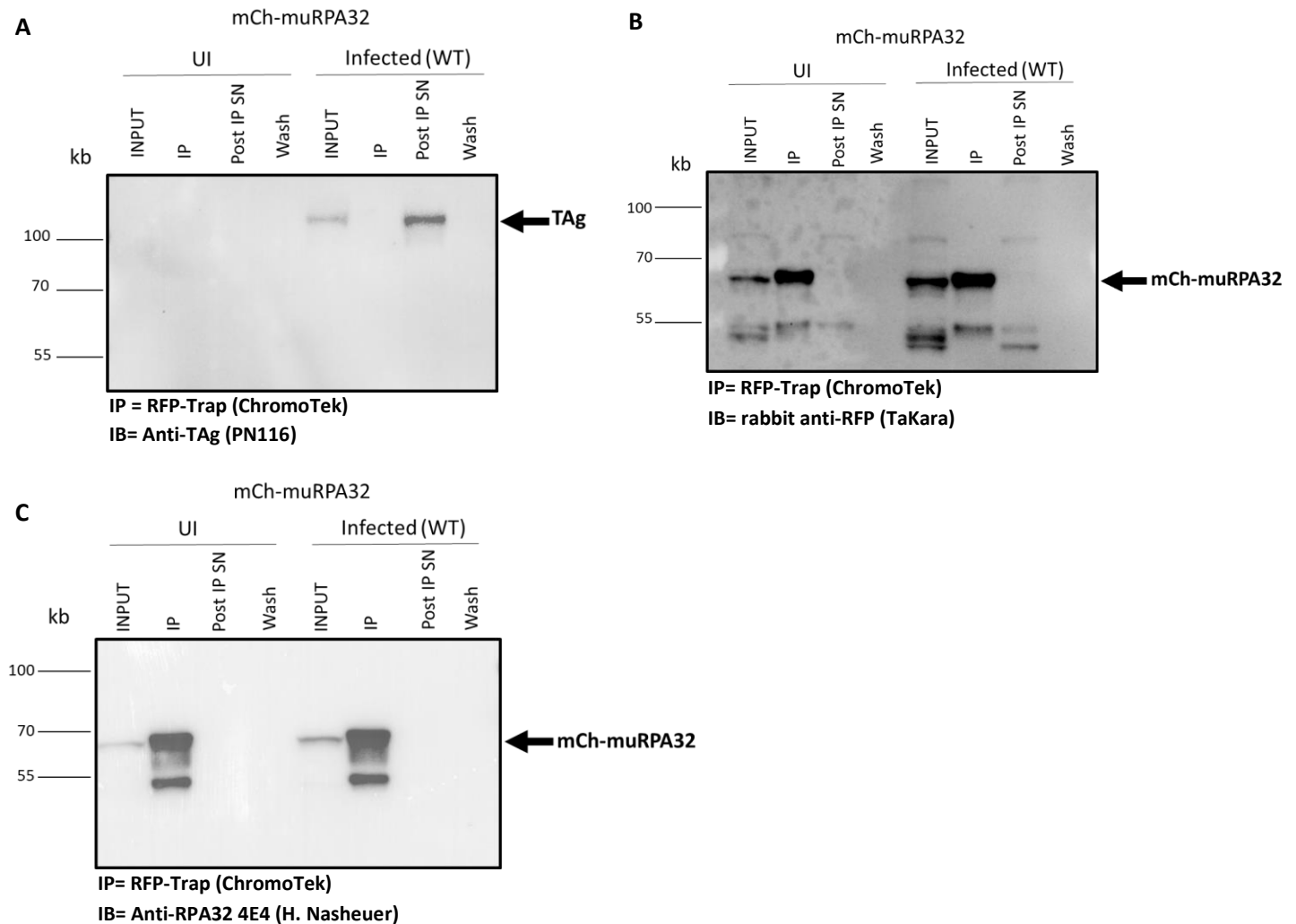
not interact and co-IP with the target protein.



**Figure 10:  LT does not co-immunoprecipitate with mCh-muRPA32.**  C57 cells stably expressing mCh-muRPA32 were infected with NG59RA.  At 30 hpi, cells were lysed, and RFP-trap was used to immunoprecipitate. Samples were analyzed by immunoblot with antibodies indicated. Blot **A** was blotted and imaged, the antibodies stripped, the blot and re-probed as indicated **(B).  (A)** Samples IP'd using RFP-trap and blotted with anti-TAg antibody **(B)**.  Blot A was stripped and re-probed with anti-RFP **(C)** Samples were IP'd using RFP-trap and blotted for with anti-RPA32 antibody.  INPUT= 5% of the whole lysate, IP= final precipitated protein, POST IP SN= supernatant following IP incubation, WASH= first Lysis Buffer wash of Ab-bead complexes after supernatant removal.

Samples using either LT or RFP-trap bead complexes bound to their target protein as determined by immunoblot (**Figure 9B, 10B**).  Additionally, RFP-trap UI and infected samples had visible protein when blotted with either anti-RPA32 or anti-mCherry (**Figure 10-B, C**).  Both the "POST IP SN" and "WASH" lanes of showed little to no mCh-muRPA32 signal, indicating that the RFP-Trap efficiently IPs the mCh-muRPA32 protein.

## Discussion:

Polyomaviruses are dsDNA viruses that hijack host DDR response proteins to effectively replicate their genomes.  The viral protein large T-antigen (LT) is essential for vDNA replication and is believed to interact with a variety of host DDR proteins to facilitate the viral life cycle (Fanning et al., 2009; Heiser et al., 2016; Topalis et al., 2013).  One such protein complex, called replication protein a (RPA) has been shown to accumulate at sites of vDNA replication, and possibly interact directly with LT (Banerjee et al., 2013; Ning et al., 2015).  This study sought to determine the interaction of LT and RPA32, using the single and double nucleotide LT mutants E320A, K308E, E320A+K308E.  Both single mutants were shown previously to have LT-RPA binding in the context of inducible plasmid transfections within human-based cell lines through co-immunoprecipitation (Banerjee et al., 2013).  A murine model using transfected viral genomes offers a more accurate look into the interactions of these proteins.  We wished to determine if co-immunoprecipitation of RPA32 and LT was possible in the context of infection, with hopes of characterizing the differences seen in each of the three LT mutants.

TAg expression was seen when cells were transfected with linear viral DNA.  Due to the time constraints of this study, we were unable to test any differences in transfection efficiency between linearized and re-ligated (circular) vDNA.  Moving forward, it may prove worthwhile to explore this difference, if any, as it could offer insights into how better to transfect cells in the future.  It is possible that re-circularized vDNA, which is more similar to uncoated vDNA during an infection, may lead to a better overall replication of the virus within cells.

Analysis of vDNA replication within transfected cells was an important step in identifying if LT mutants, which supposedly do not bind RPA, could replicate their own genome.  While prior research on E320A pointed towards an increase in overall vDNA replication, it unknown whether K308E would behave in the same manner.  Additionally, the double-mutant E320A+K308E may have resulted in a completely non-functional TAg, which could prevent any

level of vDNA replication. Using Hirt DNA isolation and gel analysis, we found that all mutants were able to replicate vDNA. While no vDNA was visible in all E320A samples, it is possible that vDNA replication occurred, but was at a level much smaller compared to the other mutants and was therefore 'lost' in their signal. No difference was seen between increasing amounts of transfected vDNA, and bands were qualitatively comparable to WT. However, due to the constraints of this study, we were unable to analyze vDNA replication from a quantitative standpoint. While all bands may appear similar, it is possible that each LT mutant results in differing levels of vDNA replication; in this way the double-mutant E320A+K308E could replicate lower levels of vDNA, being more hindered by two mutations in its RPA-binding region. To explore the exact differences in these mutants, compared to WT MPyV, a more in-depth quantitative analysis such as quantitative-Polymerase Chain Reaction (q-PCR) could be completed on each band isolated from the DNA gel.

We did not observe co-immunoprecipitation of LT and RPA32 in the context of WT infections. While this binding relationship in WT MPyV was observed in the Banerjee experiments, we were unable to replicate their results when using mouse fibroblasts and infecting. The previous study indicated that RPA70 and LT could be co-immunoprecipitate with one another when using WT LT, but such an interaction was not present when using each LT mutant (Banerjee et al., 2013). This led the authors to conclude that MPyV LT directly binds to RPA, and that the amino acid residues explored were essential for this interaction. The differences between our results and those reported in Banerjee, et. al. may be due to the cell type used, the RPA protein used, or the overexpression of LT in their experiments.

Specifically, the Banerjee study used expression plasmids for either LT (and mutants) or GFP-RPA70 in different cell types. Plasmids expressing either GFP-RPA70 and LT (and mutants) were co-transfected into HEK293 cells. These cells are of human origin, and therefore are not completely representative of the cellular environment during MPyV infection. This may

result host-virus protein interactions in mice which may not occur in the human model, resulting in an inability of RPA and LT to interact with one another on the level seen in the Banerjee IP's. Alternatively, the RPA70 used in the Banerjee study was of human origin, therefore it is possible that species differences between the RPA proteins could contribute to interactions. However, we also examined lysates from infected C57 cells that stably expressed a mCherry-tagged human RPA32 protein (mCh-hsRPA32), with results similar to experiments performed with mCh-muRPA32. The fact that they chose RPA70 for their studies and we used RPA32 may also explain the different outcomes we observed. However, previous, unpublished results from our lab did not detect an interaction with LT when we used the same GFP-hsRPA70 construct described in the Banerjee paper (Kim Erickson, unpublished data). Therefore, while the species of RPA may not affect LT interaction with RPA, the cell background may contribute to differences seen between the two studies.

The Banerjee study did investigate the interaction of LT and RPA in the context of mouse cells. However, the mouse fibroblast cells used were stably expressing an tet-inducible LT, meaning expression of the LT protein is controlled by the addition or removal of doxycline. While the cell background is in mouse cells, LT is expressed from the CMV promoter at much higher levels than seen during infection. Thus, the inducible LT does not accurately simulate the normal cellular environment upon MPyV infection. It is possible that the results seen in the Banerjee study are due to an over-expression of both RPA and LT in the cell, essentially forcing an interaction between the two proteins and allowing them to co-precipitate one another. While our study utilized mouse fibroblasts that stably expressed a fluorescently labeled RPA32 protein at higher levels than endogenous, untagged RPA32, we examined the interaction of LT and RPA from two vantage points. We immunoprecipitated with either antibodies to LT or the mCherry tag and did not see an interaction in either case. Co-immunoprecipitation experiments

were performed in the context of viral infection, therefore decreasing the likelihood of overexpression and any 'forced' interactions between RPA32 and LT that may result.

The inability to co-immunoprecipitate RPA32 and LT seen in our experiments may be due to a 'numbers game', where interactions are occurring, but at such a low level that we are unable to visualize using immunoblots.  Our inability to visualize an interaction by immunoblot may represent limitations of the experimental techniques.  While an interaction is occurring, and levels of RPA-LT complexes are present in the final IP they may be below the limit of detection for the antibody used.  Banerjee's experiments may therefore increase the amount of interaction to a level that is ultimately detected with immuno-blotting.  This could also be because our experimental model is set in the context of infection, where full viral genomes are being replicated and transcribed as opposed to a single protein.  The lysates used in each IP were from cells expressing all viral proteins, in the hopes of examining the RPA-LT interaction in a more accurate context.  While LT and RPA may interact when they are the only proteins around, it is likely that in the context of MPyV infection, other viral and host proteins are also interacting with LT/RPA.  It is known that many different DDR proteins play a role in vDNA replication; therefore, other DDR protein interactions may result in a less obvious interaction of RPA and LT when assisting vDNA replication.

Finally, it is possible that our data may support high-resolution microscopy data from our lab, where we observe separation of LT and mCh-RPA32 in vDNA replication centers during infection.  SIM microscopy looking to characterize polyoma replication centers shows that both TAg and RPA are recruited to sites of vDNA synthesis (**Figure 11**) (Garcea Lab, unpublished). While RPA and TAg both appear in these replication centers, they appear to be spatially separate from one another, with only a small population colocalizing (Garcea Lab, unpublished). It is possible that while both proteins are essential for efficient vDNA replication, they may localize to different regions/subdomains of replication complexes.  Additionally, EdU pulse-

chase labeling of replicating vDNA indicates the movement of vDNA from the LT site to the

RPA32 sites.  Thus, our co-immunoprecipitation data support the idea that these complexes are

spatially and functionally separate from one another during viral infection.
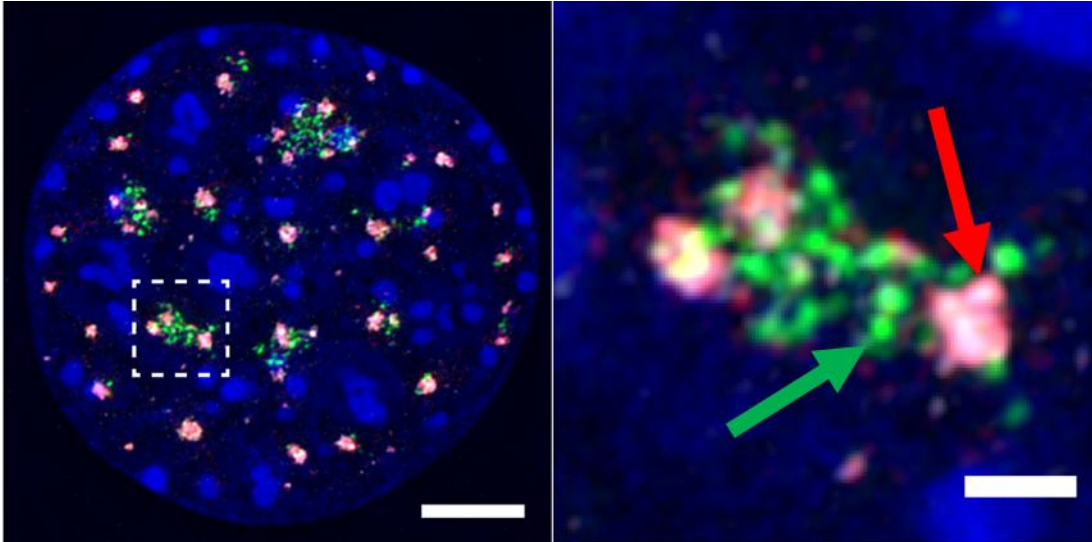


**Figure 11: Nikon Structured Illumination Microscopy (N-SIM) of C57 MEF infected with NG59RA for 28 hours**.  Cells were pulsed with EdU to label replicating vDNA. Blue = DAPI, Green (arrow) = GFP-RPA32, Red (arrow) = viral T-Antigen, White = EdU (nascent DNA). Scale Bars: Top = 5um, Bottom = 1um. (Doug Peters, Garcea Lab, unpublished).

The initial goal of this study was to characterize each of three LT mutants in the context

of RPA32 binding.  However, due to unforeseen time constraints and the inability to co-

immunoprecipitate RPA and LT from WT infections, we were unable to experiment with these

mutants beyond vDNA replication.

## Acknowledgements

I would like to thank first and foremost the entire Garcea Lab for their mentorship and support over the course of this project, and for the creating of a positive and fun lab environment. Secondly, I'd like to thank Dr. Robert Garcea for allowing me the opportunity to complete research within his lab, and for an overarching guidance throughout my project. I'd also like to give a special thanks to Kim Erickson who provided mentorship, and who taught me the ins and outs of the lab and protocols. Without her support and insight, I would not have been able to learn or grow as much as I have in my time working in a virology lab, and I am extremely grateful for her patience. I would also like to thank Doug Peters for supplying SIM images and figures of MPyV replication centers. I also acknowledge the Sawyer Lab, who shared the use of their equipment, allowing for my research to progress. Finally, I want to thank my thesis committee, Dr. Robert Garcea, Dr. Christy Fillman, and Dr. Valerie McKenzie for their time and input.

## References:

Ahsan, N., & Shah, K. V. (2006). Polyomaviruses and human diseases. *Advances in Experimental Medicine and Biology*, *577*, 1–18. https://doi.org/10.1007/0-387-32957-9_1

Banerjee, P., deJesus, R., Gjoerup, O., & Schaffhausen, B. S. (2013). Viral Interference with DNA Repair by Targeting of the Single-Stranded DNA Binding Protein RPA. *PLoS Pathogens*, *9*(10). https://doi.org/10.1371/journal.ppat.1003725

Brodsky, J. L., & Pipas, J. M. (1998). Polyomavirus T Antigens: Molecular Chaperones for Multiprotein Complexes. *Journal of Virology*, *72*(7), 5329–5334.

Fanning, E., Klimovich, V., & Nager, A. R. (2006). A dynamic model for replication protein A (RPA) function in DNA processing pathways. *Nucleic Acids Research*, *34*(15), 4126–4137. https://doi.org/10.1093/nar/gkl550

Fanning, E., Zhao, X., & Jiang, X. (2009). Polyomavirus Life Cycle. In B. Damania & J. M. Pipas (Eds.), *DNA Tumor Viruses* (pp. 1–24). https://doi.org/10.1007/978-0-387-68945-6_1

Heiser, K., Nicholas, C., & Garcea, R. L. (2016). Activation of DNA damage repair pathways by murine polyomavirus. *Virology*, *497*, 346–356. https://doi.org/10.1016/j.virol.2016.07.028

Hirt, B. (1967). Selective extraction of polyoma DNA from infected mouse cell cultures. *Journal of Molecular Biology*, *26*(2), 365–369. https://doi.org/10.1016/0022-2836(67)90307-5

Jackson, S. P., & Bartek, J. (2009). The DNA-damage response in human biology and disease. *Nature*, *461*(7267), 1071–1078. https://doi.org/10.1038/nature08467

Jiang, X., Klimovich, V., Arunkumar, A. I., Hysinger, E. B., Wang, Y., Ott, R. D., … Fanning, E. (2006). Structural mechanism of RPA loading on DNA during activation of a simple pre-replication complex. *The EMBO Journal*, *25*(23), 5516–5526. https://doi.org/10.1038/sj.emboj.7601432

Ning, B., Feldkamp, M. D., Cortez, D., Chazin, W. J., Friedman, K. L., & Fanning, E. (2015). Simian Virus Large T Antigen Interacts with the N-Terminal Domain of the 70 kD Subunit of Replication

Protein A in the Same Mode as Multiple DNA Damage Response Factors. *PLoS ONE*, *10*(2). https://doi.org/10.1371/journal.pone.0116093

Prado, J. C. M., Monezi, T. A., Amorim, A. T., Lino, V., Paladino, A., & Boccardo, E. (2018). Human polyomaviruses and cancer: an overview. *Clinics*, *73*(Suppl 1). https://doi.org/10.6061/clinics/2018/e558s

Stehle, T., & Harrison, S. C. (1997). High-resolution structure of a polyomavirus VP1-oligosaccharide complex: implications for assembly and receptor binding. *The EMBO Journal*, *16*(16), 5139– 5148. https://doi.org/10.1093/emboj/16.16.5139

Sullivan, C. S., & Pipas, J. M. (2002). T Antigens of Simian Virus 40: Molecular Chaperones for Viral Replication and Tumorigenesis. *Microbiology and Molecular Biology Reviews*, *66*(2), 179–202. https://doi.org/10.1128/MMBR.66.2.179-202.2002

Topalis, D., Andrei, G., & Snoeck, R. (2013). The large tumor antigen: A "Swiss Army knife" protein possessing the functions required for the polyomavirus life cycle. *Antiviral Research*, *97*(2), 122– 136. https://doi.org/10.1016/j.antiviral.2012.11.007

Whalen, K. A., de Jesus, R., Kean, J. A., & Schaffhausen, B. S. (2005). Genetic Analysis of the Polyomavirus DnaJ Domain. *Journal of Virology*, *79*(15), 9982–9990. https://doi.org/10.1128/JVI.79.15.9982- 9990.2005

Wold, M. S. (1997). Replication Protein A: A Heterotrimeric, Single-Stranded DNA-Binding Protein Required for Eukaryotic DNA Metabolism. *Annual Review of Biochemistry*, *66*(1), 61–92. https://doi.org/10.1146/annurev.biochem.66.1.61